Biomass Conversion and Biorefinery (2024) 14:1405–1412
https://doi.org/10.1007/s13399-023-05187-5

ORIGINAL ARTICLE

Impact of stainless steel nano-alloys on biogas production rate: safe catalysts

Sara El-Ansary[1] · Mahmoud A. Sliem[2] · Yehia Badr[1] · Wafaa Soliman[1]

Received: 23 August 2023 / Revised: 17 November 2023 / Accepted: 27 November 2023 / Published online: 22 December 2023

Keywords Resonance fluorescence · Stainless steel nano-alloys · Biogas production rate · New catalysts

1 Introduction

Looking for renewable energy sources as a result of the depletion of fossil energy sources is a critical issue. Recent innovations are looking for safe, clean, and low-cost solutions. Biogas is considered a renewable and clean source of energy. The enhancement of its production depends on stimulating microbial activity with different kinds of organic and inorganic additives. The organic additives include biological additives (weeds, plants [1], crop residues, microbial cultures, etc.) and strains of some bacteria and fungi (by stimulating the activity of particular enzymes [2]).

However, inorganic additives are heavy metals. It is reported that the plant with a higher content of heavy metals (Cu, Co, Fe, Ni, Cr, and Zn) produced a higher yield of CH_4 [3–6]. Ni-dependent metallo-enzymes enhanced the biogas rate up to 54%. However, nickel ions are used in the form of salts, and the effects of their anions were not taken into account [7]. Fe_3O_4 nanoparticles (the source of Fe^{+2} ions [8]) with a concentration below the toxicity limit enhanced the biogas production due to the ability of iron to lose or gain electrons during the anaerobic digestion (AD) process [9]. Zero-valent iron (ZVI) nanoparticles (NPs), as electron donors, increase the biogas production rate via the high amount of hydrogen produced upon the dissolution of the ZVI nanoparticles [10, 11]. Co, Ni, and Pt are promising enhancers for biogas and methane production during the AD process [12–14].

However, some metal or metal oxide nanoparticles are reported as inhibitors in spite of their size and concentrations. For instance, CuO nanoparticles decrease the hydraulic retention time (HRT) [15]. ZnO [16], Ag, Cu, Pd, TiO_2, SiO_2, Al_2O_3, CeO_2, and Fe_2O_3 are inhibitors [17] because of their toxic effect on the anaerobic bacteria.

Moreover, Cr ions act as an inhibitor factor for biogas production [18–20] as Cr in the +6 oxidation state is known to be carcinogenic and mutagenic. It is used as a wood preservative and is well documented to have a high toxicity effect on aquatic organisms [21]. However, if it is reduced to a +3 oxidation state, it may be significantly safer [22]. Recently, stainless steel–based Cr quantum dots (QDs) were synthesized by laser ablation in distilled water to treat carcinoma in an in vitro study. The low concentration, the purity of the colloidal solution, and the valence of Cr (+3) excluded the toxicity of QDs and attributed the efficient treatment to its near-infrared (NIR) resonance fluorescence as different mechanisms [22]. In addition, the smaller particle size provides a larger surface area. The stainless steel target used in that study was commercial, i.e., the random distribution of its elements is highly probable [23].

This work investigates the viability of nontoxic stainless steel colloidal solutions for the application of biogas production. Some results are compared with previously work [24], since their biodigesters are treated simultaneously considering the same experimental and environmental conditions. In addition, biological effect is interpreted based on the biogas flame and available data. As a new finding, the free of Cr stainless steel colloidal solution produces unexpected biogas volume 207% of control. In addition, Cr-based stainless nano-alloys exhibit eco-friendly inhibition effect.

✉ Wafaa Soliman
wafaamas@cu.edu.eg

[1] Departmet of Laser Sciences and Interactions, National Institute of Laser Enhanced Sciences (N.I.L.E.S), Cairo University, Giza 12613, Egypt

[2] Department of Laser Applications in Metrology, Photochemistry and Agriculture, National Institute of Laser Enhanced Sciences (N.I.L.E.S), Cairo University, Giza 12613, Egypt

2 Experimental work

2.1 Synthesis of stainless steel nano-alloys

Commercial stainless target (1 cm × 1 cm × 2 mm) steel was rinsed with ethanol and distilled water to remove impurities from its surface. X-ray diffraction spectrometer (XRD), energy-dispersive analysis, X-ray diffraction (EDAX), and X-ray fluorescence (XRF) measurements determined that the target belongs to stainless steel 304 and consists mainly of Fe, Ni, and Cr. The elements of the target, according to XRF, are listed in Table 1. A Nd:YAG laser ($\lambda = 355$ nm, $\tau = 8$ ns, rep. rate = 10 Hz), operated at 19, 26, and 60 mJ/pulse and focused by a lens of 20 cm focal length, was used to ablate the target under 5 cm^3 of distilled water. The target was ablated for 30 min and scanned manually during ablation. Nano-alloys are collected in the form of colloidal solutions and sonicated frequently to prevent aggregation.

2.2 Biogas

The substrate material is cattle dung, where it is abundant throughout the year and cheap; besides, it can be used as a fertilizer. A fresh cow dung sample (~ 10 kg) was collected from the Western Farm of the Faculty of Agriculture, Cairo University, Egypt. The sample was added to distilled water (8 L) and homogenized for 60 min for the slurry preparation. The total solids of the fresh manure, the slurry, and the volatile content of the slurry were 13.6, 7.8, and 80.36%, respectively.

The anaerobic system used was built from special bench-scale digesters [13, 14]. The system consisted of 15 biodigesters, a water bath to control the temperature at 37 ± 0.5 °C, gas outlets, valves, a water trap, and graduated cylinders. Each biodigester (as a separate unit with all components connected in series) consisted of Pyrex® round media storage bottles (1000 mL for each) with a gas outlet connected to the biogas holder. Two air valves were inserted: one before the biogas holder to maintain the anaerobic digestion condition during measurements as pressure control, and the other one after the biogas holder to connect with the biogas analyzer. The pH of the cow dung sample was 7. The volume of the biogas produced was measured using the liquid displacement from an ultra-clear polypropylene cylinder (1000 ± 10 mL, Azlon, Staffordshire, UK). The cylinder was placed upside down in another one (2000 mL, Azlon) filled with a colored water to ensure an accurate reading of the biogas volume.

The anaerobic digestion of cow dung treated with 100 ppm of $NiFe_2O_4$ prepared by the co-precipitation method in the previous work [24] and of three samples of stainless steel nano-alloys (synthesized by laser powers of 19, 26, and 60 mJ/pulse with 10 mL for each) was examined individually. Three replications for the control and each treatment were studied. The total volume of each digester was 1000 mL, with a working volume of 800 mL, and a remaining space was left for gas holding. The incubation period was 50 days, and biogas yield was measured every 24 h.

Table 1 Composition of the commercial stainless steel target, according to XRF [23]

Analyte	Mass fraction (%)
C	*0.100*
Si	*0.447*
P	*0.028*
S	*0.003*
V	*0.097*
Cr	*19.456*
Ni	*9.085*
Cu	*0.205*
Mo	*0.149*
Mn	*1.477*
Fe	*Balance*

3 Results and discussion

3.1 Properties of stainless steel nano-alloys

The mass of material ejected from the target is estimated assuming a cone-shaped ablation volume [25]. This mass is used to determine the nano-alloy concentrations per mL of liquid presented in Table 2. The composition of the nano-alloys synthesized at 19, 26, and 60 mJ/pulse was examined by EDAX for elemental investigations, and an XRD spectrometer is used to investigate the phases of nano-alloys. Nano-alloy synthesized by ablation of stainless steel at laser energy of 26 mJ/pulse did not contain Cr, as shown in Table 3, suggesting that there is no uniform distribution of Cr on the surface of the stainless steel target.

Table 2 Estimated concentration of the ejected mass by laser ablation of a stainless steel target at 19, 26, and 60 mJ/pulse

Laser energy	Concentration (μg/mL)
19 mJ/pulse	4.002×10^{-4}
26 mJ/pulse	3.4135×10^{-3}
60 mJ/pulse	1.24×10^{-2}

Table 3 EDAX of the nano-alloys synthesized by ablation of a stainless steel target at 19, 26, and 60 mJ/pulse

	Weight (%)			
	Cr	Ni	Fe	O
19 mJ/pulse	14.59	2.38	47.08	Balance
26 mJ/pulse	0	0.16	13.57	Balance
60 mJ/pulse	2.78	14.30	82.91	Balance

Figure 1 shows HRTEM images of the three samples. Figure 1a shows different sizes of spherical nano-alloys synthesized by 19 mJ/pulse in the range of 14–39 nm. The Fabry–Perot diffraction patterns suggest that the particles are weak crystallite since the inset figure shows bright spots instead of bright circles. Figure 1b shows rod-shaped nano-alloys in the size range of 13–60 nm synthesized by 26 mJ/pulse, and Fig. 1c shows spherical nano-alloys in the size range of 10–19 synthesized by 60 mJ/pulse. Silva et al. [26, 27] reported the formation of different Fe_2O_3 nanostructures, including nanowires, nanosheets, nanobelts, and nanoribbles, by ablating Fe nanoparticles in methanol and using UV irradiation (248 nm) for annealing. The shape of nanostructures was transformed into nanowires by increasing the ablation time and number of laser shots.

Figure 2a shows the XRD pattern of samples synthesized by 19 mJ/pulse and includes two weak peaks corresponding to the Fabry–Perot diffraction patterns. Table 4 lists all the peaks for the three ablated laser energies. Further studies were made using profile matching with constant scale factor using the Fullprof Suite software package, which was based on comparison of the XRD data of nano-alloys with the data obtained from reference cards of FeO and $FeO{\cdot}Cr_2O_3$, where their matching has the highest probability. The reference cards belong to an X-ray diffraction spectrometer (Empyrean, Panalytical, Elmelo, Netherlands, with a copper target). Figure 2b shows the comparison between the peak lists of experimental data at 19 mJ/pulse and both of the FeO and $FeO{\cdot}Cr_2O_3$ cards for assignment. In addition, the comparison assigns some peaks to other samples, according to the list in Table 4. The comparison indicates that the samples, prepared at 19 and 60 mJ/pulse, are a mixture of nano-alloys and contain Cr in their composition. However, the sample prepared at 26 mJ/pulse is free of Cr, confirming the data shown in Table 3.

Regarding Ni, the comparison does not neglect the existence of any Ni compounds, contradicting the data listed in Table 3. However, the XRD technique requires significant amounts of stainless steel nano-alloys for detection and accuracy [28]. In addition, the matching of the compared cards shown in Fig. 2b has the highest probability, as aforementioned, since Fe is the most abundant metallic element.

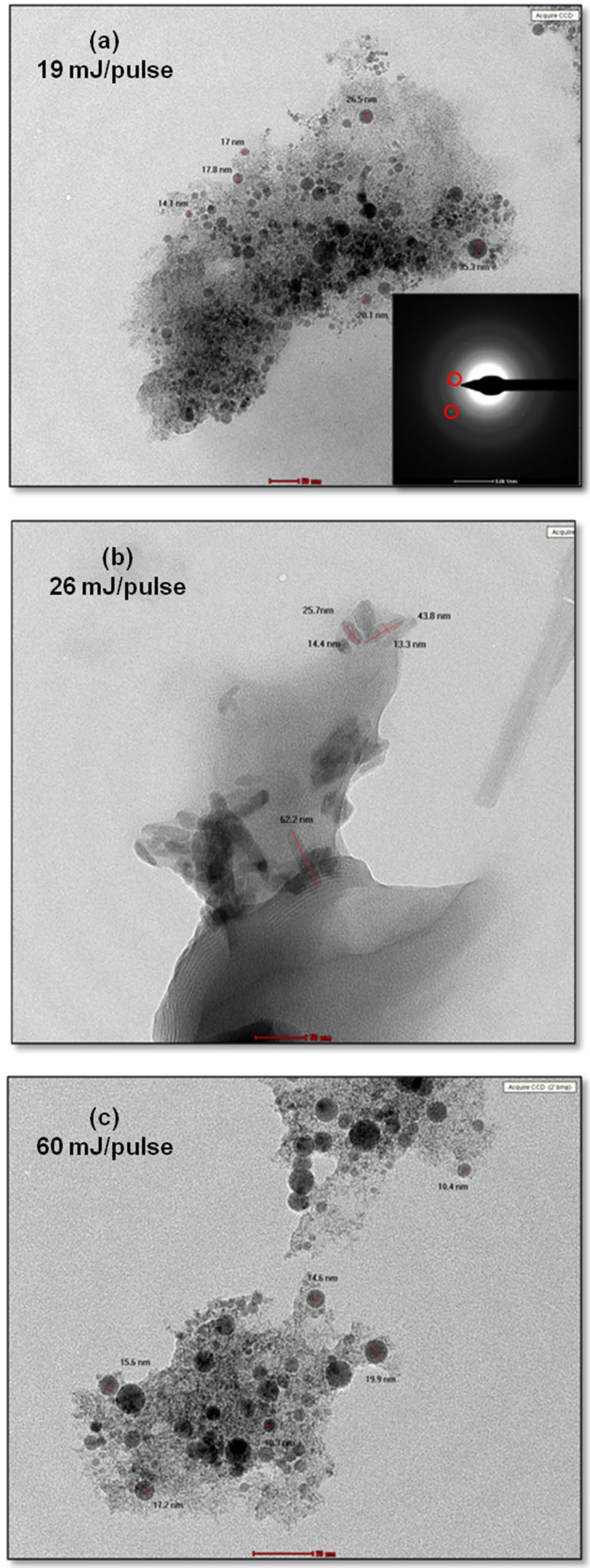

Fig. 1 HRTEM of nano-alloys synthesized by laser ablation of stainless steel in water at different laser energies

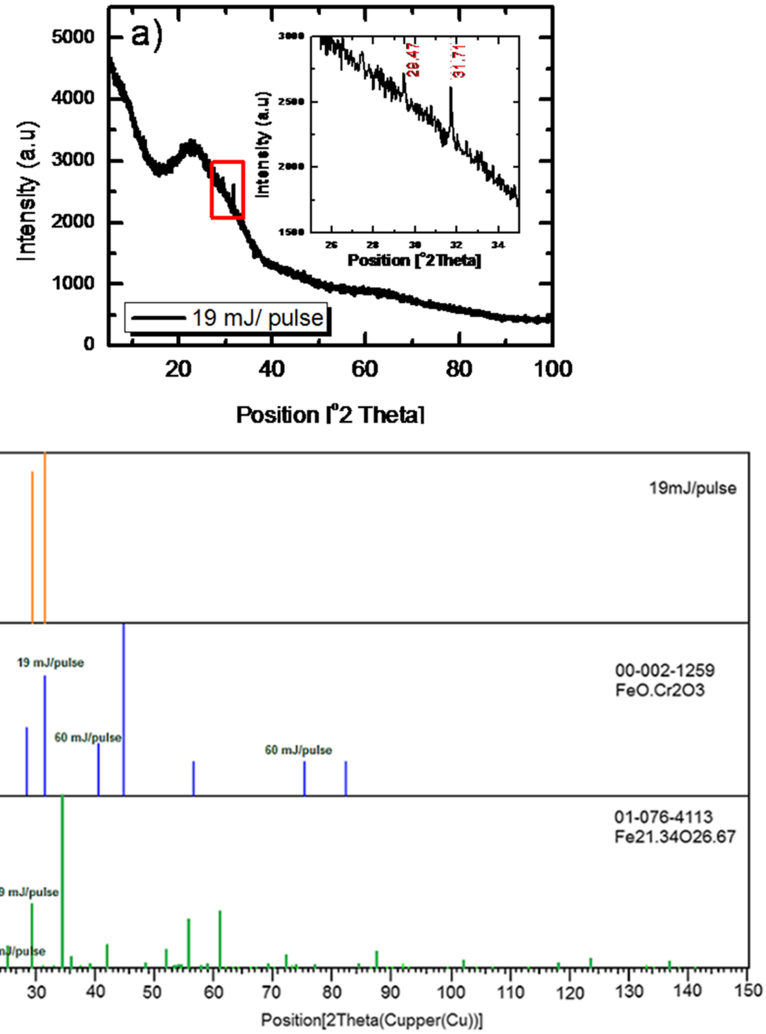

Fig. 2 XRD pattern of nano-alloys synthesized by laser ablation of a stainless steel target in water at 19 mJ/pulse: **a** measured pattern, **b** matching with reference cards

Table 4 List of XRD peaks of nano-alloys synthesized by 19, 26, and 60 mJ/pulse

	2θ(deg.)	d-spacing (Å)	FWHM (deg.)	Relative intensity (%)
(a) 19 mJ/pulse	29.4733	3.03069	0.1535	58.19
	31.7199	2.82098	0.0768	100.00
(b) 26 mJ/pulse	23.2160	3.83142	0.6140	100.00
(c) 60 mJ/pulse	10.2863	8.59993	0.8187	100.00
	12.4366	7.11743	0.6140	19.05
	15.1675	5.84154	0.9210	45.59
	27.3219	3.26425	0.9210	88.06
	36.6590	2.45146	0.8187	34.41
	37.7082	2.38563	0.6140	17.34
	39.7041	2.27018	0.7164	20.33
	62.2751	1.49090	0.6140	48.60
	74.6218	1.27188	0.8187	43.62

3.2 Effect of stainless steel nano-alloys on biogas production

Ten milliliters of stainless steel nano-composites in colloidal solutions produced by laser ablation with different laser energies (19, 26, 60 mJ/pulse) were added to cow dung. The daily biogas yields of the treated digesters and control were oscillating closely for the first 26 days, as shown in Fig. 3a. After 26 days, the daily biogas yield of the treated digester by nano-alloys synthesized by laser energy of 26 mJ/pulse was apparently enhanced. However, the biogas yields of other treated digesters were inhibited and became lower than those of the control.

The cumulative biogas produced from different treatments with stainless steel nano-alloys is shown in Fig. 3b. It is observed that the cumulative biogas of the treated sample with stainless steel nano-alloys, synthesized by laser energy of 26 mJ/pulse, increased monotonically for the first 26 days and drastically after that, producing the highest cumulative biogas volume of 4840 mL. On the other hand, the cumulative biogas yields of other treatments decreased seriously and became

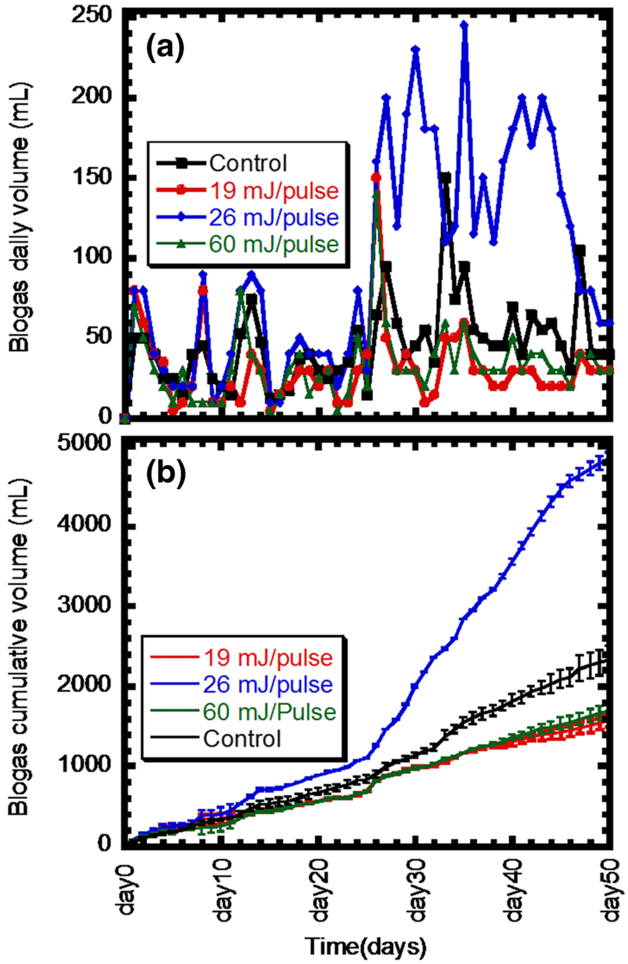

Fig. 3 **A** Daily biogas production rate of treated cow dung with nano-alloys; **b** cumulative biogas production rate of treated cow dung with nano-alloys

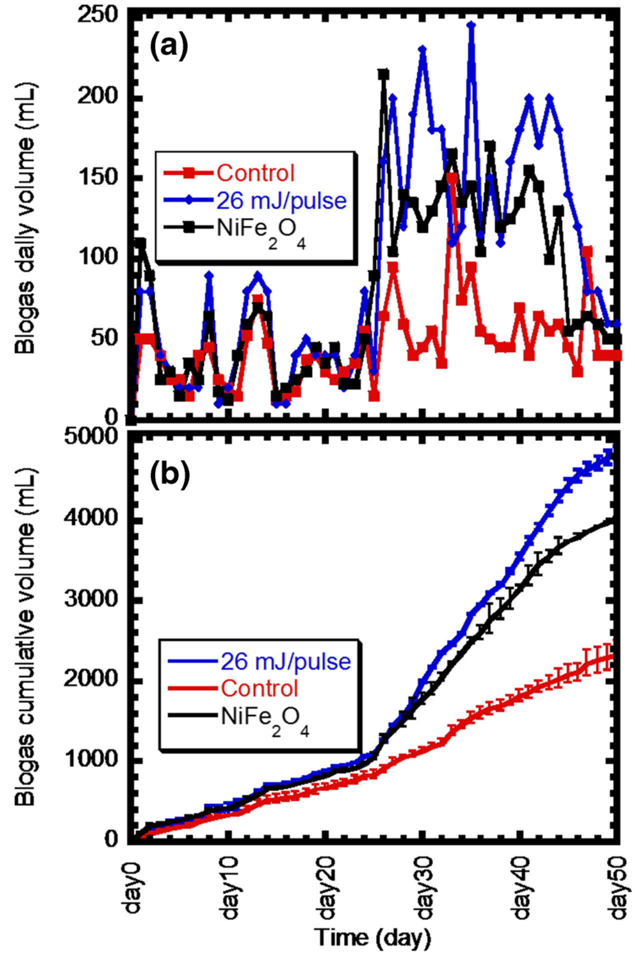

Fig. 4 Biogas production rate of cow dung treated with $NiFe_2O_4$ nanoparticles and stainless steel nano-alloys synthesized by laser energy at 26 mJ/pulse: **a** daily, **b** cumulative

lower than control (~2337.5 mL). The treated samples with stainless steel nano-alloys, synthesized by laser energy at 19 and 60 mJ/pulse, produced cumulative biogas yields of 1575 and 1690 mL, respectively.

In our work, the stainless steel nano-alloys synthesized by laser ablation with laser energies (19 and 60 mJ/pulse) contained Cr in oxidation state + 3 and seem inhibitory to an extent, in spite of their low concentration. However, the nano-alloys, obtained from stainless steel ablated at 26 mJ/pulse, seem to be enhancers. So, we believe that the enhancement of biogas production is attributed to many reasons, like the absence of Cr and the different shape of the nano-alloys compared to the others.

3.3 Comparison study between the effects of ferrite nanoparticles and stainless steel nano-alloys on biogas production

Figure 4 shows a comparison between the biogas production rates of digesters treated with $NiFe_2O_4$ nanoparticles and the nano-alloys obtained from stainless steel ablated with laser energy of 26 mJ/pulse as these nano-alloys contain mainly Ni and Fe elements. The synthesis and characterization of $NiFe_2O_4$ nanoparticles are reported in previous work [24]. Figure 4a shows that both the $NiFe_2O_4$ nanoparticles and stainless steel nano-alloys enhance biogas production significantly. However, the effect of stainless steel nanoalloy was found to be much greater. In addition, Fig. 4a shows that the maximum biogas production per day for the digester treated with $NiFe_2O_4$ nanoparticles on day 26 was 215 mL, while the maximum biogas production per day for the digester with stainless steel nano-alloys on day 35 was 245 mL.

Figure 4b shows that the cumulative biogas production of stainless steel nano-alloys (4840 mL) exceeds that of $NiFe_2O_4$ nanoparticles (4020 mL). Although both nano-alloys and $NiFe_2O_4$ nanoparticles mainly have the same metal element, the treatment of biogas digesters with nano-alloys shows a higher enhancement of production than that treated with $NiFe_2O_4$ nanoparticles. We attribute this to several reasons: the stainless steel nano-alloys were more pure than the prepared $NiFe_2O_4$ nanoparticles, as in liquid-phase laser ablation there are no byproducts, whereas in chemical preparation, even if we wash the precipitate several times, we cannot guarantee 100% removal of the byproducts. Also, the concentration of the added $NiFe_2O_4$ nanoparticles may not be the optimum concentration, as we added 100 ppm of $NiFe_2O_4$, but the yield of the nano-alloys from the stainless steel was too weak. The enhancement of biogas production in digesters treated with nano-alloys may also be attributed to the different shape of the nanoalloy (nanorod) than the $NiFe_2O_4$ nanoparticles (nanosphere). The error bars and cumulative volumes shown in Figs. 3 and 4 are estimated based on the standard deviation and the average of replications, respectively. It is noticed that the error bars have the same range, indicating the reliability of he measurements.

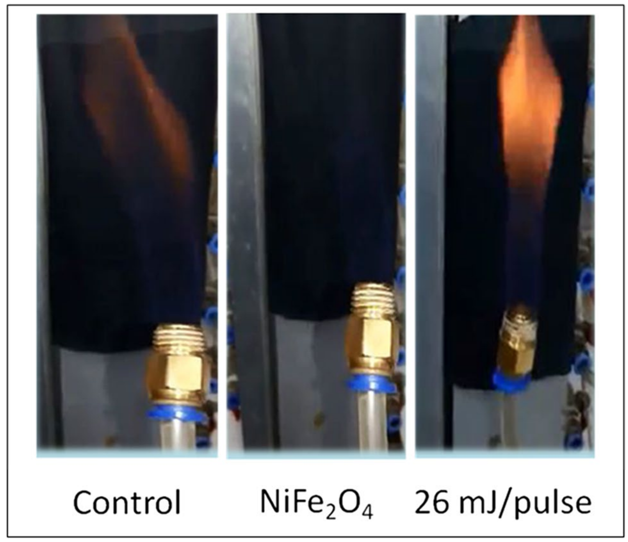

Fig. 5 Biogas flames of control, $NiFe_2O_4$, and stainless steel biodigesters

3.4 fluorescence of stainless steel nano-alloys: suggested inhibition's mechanism

Recently, we synthesized stainless steel–based Cr QDs by laser ablation of a commercial target in distilled water to treat laryngeal carcinoma in a vitro study. The carcinoma was treated without using a laser or powerful magnets for phototherapy. The low concentration, the purity of the colloidal solution, and the valence of Cr (+3) excluded the toxicity of QDs and attributed the efficient treatment to its near-infrared (NIR) resonance fluorescence [22]. It is supposed that not only QDs have the ability to absorb the NIR energy required for excitation from the surrounding medium since lasers or optical sources are not used for excitation, but also that the fluorescence of QDs is a resource for heat shock mechanisms. In addition, we supposed that the low percentage of QDs allowed the deep penetration of NIR light inside cancer cells [29].

In this study, we synthesized stainless steel–based Cr nano-alloys by laser ablation using the same target to examine the effect of this strategy on the anaerobic digestion process for biogas production. The significant suppression in the biogas production rate strongly supports the heat shock mechanism of stainless steel–based Cr nano-alloys. Also, it infers that the heat shock may disrupt and damage the anaerobic bacteria or limit, at least, their differentiation.

3.5 Efficient treatment

Both the biogas flame and the production rate may indicate an efficient treatment. Regarding the biogas flame, it was detected weakly. No flame was obtained at the first week due to the low pressure of biogas [30]; however, by the second week, the flame was obtained. Figure 5 shows the biogas flames for both the control digester and biodigesters that were treated with $NiFe_2O_4$ and stainless steel nano-alloys after 50 days, conforming to Fig. 4. Both the flames of the control and stainless steel biodigesters have a blue-reddish color, indicating a mixture of methane and carbon dioxide. However, the $NiFe_2O_4$ digester has only a blue color, indicating a high percentage of methane due to the significant growth of methanogenesis bacteria. Based on Table 2, the oxygen percentage in nano-alloys synthesized by 26 mJ/pulse exceeds 86% and works against the growth of methanogenesis bacteria. In methanogenesis, the terminal electron acceptor is carbon, not oxygen, depending on the pathway: $CO_2 + 4\,H_2 \rightarrow CH_4 + 2\,H_2O$. Thus, optimizing the concentration of stainless steel nano-alloys or the long incubation period is required for the significant growth of methanogenesis bacteria.

Regarding gas production rate, the 207% cumulative volume of control is relatively high in comparison to recent literature focusing on the effects of other metallic nanoparticles. Typically, Abdelwahab et al. [31] studied the impact of different concentrations (15, 30, and 60 mg/L) of Fe NPs on biogas production and effluent chemical composition from the AD of cattle manure compared with cattle manure alone. The results reveal that the highest biogas production reaches 162% of control by using 15 mg/L Fe NPs.

Akar et al. [32] studied the use of trimetallic Sn–Mn–Fe nanoparticles, recovered from waste-printed circuit boards, to enhance the quality and productivity of the anaerobic digestion (AD) of cow manure as an organic substrate.

Various concentrations (20, 50, and 100 mg/L) of the tri-metallic Sn–Mn–Fe nanoparticles were added to the biogas reactors, which were made of 1000-mL autoclave glass bottles to host the animal waste during the AD process. The pressure of the biogas produced was monitored daily for 45 days as retention time, and the volume of the produced biogas was calculated at a constant temperature (15 °C) and pressure (1.013 bar). The best biogas-producing digester (20 mg/L) revealed the highest performance, with a 113.6% enhancement in biogas production.

Kaskun et al. [33] investigated the biogas production activity by adding two concentrations (0.03 mg/L and 0.06 mg/L) of mica particles (MP) and SnO_2 NPs-doped mica ($MSnO_2$) prepared by co-precipitation. The highest biogas production yield was obtained by using 0.03 mg/L $MSnO_2$, reaching 18.1% of the control.

Considering the same experimental condition and metallic constituents, $NiFe_2O_4$ produced a gas cumulative volume of 83% of what was produced by stainless steel nano-alloys, as discussed previously.

4 Conclusion

This research investigates the viability of producing biogas from nontoxic stainless steel colloidal solutions made by laser ablation in distilled water. Part of the results is compared with previous work on $NiFe_2O_4$, since their biodigesters are treated simultaneously under the same experimental and environmental conditions. The $NiFe_2O_4$ and stainless steel nano-alloys' cumulative gas volume consequently rose to 172% and 207%, respectively, following the 50-day incubation period. To further analyze the biological effect, the biogas flame and the available data are utilized. A sudden biogas volume of 207% of control is obtained from the free Cr stainless steel colloidal solution, as reported recently. The inhibition of stainless steel digesters based on Cr, however, is ascribed to the heat shock mechanism-based NIR resonance fluorescence property.

Author contribution This work is a part of M.Sc. thesis of the author S.E. Herein, the contribution of each author:

S.E. (student): experiment, imaging, analysis, writing and editing.

M.A.S. (supervisor): revision and discussion.

Y.B. (supervisor): idea, experiment, analysis, editing, revision, and discussion.

W.S. (supervisor): experiment, imaging, analysis, writing, editing, revision, and discussion.

Funding Open access funding provided by The Science, Technology & Innovation Funding Authority (STDF) in cooperation with The Egyptian Knowledge Bank (EKB).

Data availability Data will be made available on reasonable reason.

Declarations

Ethical approval Not applicable.

Competing interests Not applicable.

References

1. NallathambiGunaseelan V (1987) Parthenium as an additive with cattle manure in biogas production. Biol Wastes 21:195–202
2. Rashid Mia Md Abdu et al (2016) Enhancement of biogas production by cellulytic bacteria from bagasse using methanogenesis. Am J Chem Biochem Eng 1:15–20
3. Hassaneen FY, Abdallah MS, Ahmed N, Taha MM, AbdElAziz SMM, El-Mokhtar MA, Badary MS, Allam NK (2020) Innovative nanocomposite formulations for enhancing biogas and biofertilizers production from anaerobic digestion of organic waste. Bioresour Technol 309:123350
4. Abdelwahab TAM, Mohanty MK, Sahoo PK, Behera D (2020) Impact of iron nanoparticles on biogas production and effluent chemical composition from anaerobic digestion of cattle manure. Bioref Biomass Conv. https://doi.org/10.1007/s13399-020-00985-7
5. Salama AM, Helmy EA, Abd El-ghany TM, Ganash M (2020) Nickel oxide nanoparticles application for enhancing biogas production using certain wastewater bacteria and aquatic macrophytes biomass. Waste Biomass Valor. https://doi.org/10.1007/s12649-020-01144-9
6. Ugwu SN, Enweremadu CC (2020) Enhancement of biogas production process from biomass wastes using iron-based additives:types, impacts, and implications. Energy Sources Part A. https://doi.org/10.1080/15567036.2020.1788675
7. Geeta GS, Jagadeesh KS, Reddy TKR (1990) Nickel as an accelerator of biogas production in water hyacinth (eichornia crassipes solms.). Biomass 21:157–161
8. Sai Ram M, Singh L, Suryanarayana MVS, Alam SI (2000) Effect of iron, nickel and cobalt on bacterial activity and dynamics during anaerobic oxidation of organic matter. Water, Air, Soil Pollution 117:305–312
9. Casals E, Barrena R, García A, González E, Delgado L, Busquets-Fité M, Font X, Arbiol J, Glatzel P, Kvashnina K, Sánchez A, Puntes V (2014) Programmed iron oxide nanoparticles disintegration in anaerobic digesters boosts biogas production. Small 10:2801–2808
10. Karri S, Sierra-Alvarez R, Field JA (2005) Zero valent iron as an electron-donor for methanogenesis and sulfate reduction in anaerobic sludge. Biotech Bioeng 92:810–819
11. Xiu Z-M, Jin Z-H, Li T-L, Mahendra S, Lowry GV, Alvarez PJJ (2010) Effects of nano- scale zero-valent iron particles on

a mixed culture dechlorinating trichlor- oethylene. Bioresource Tech 101:1141–1146
12. Al-Ahmad A, Hiligsmann S, Delvigne F, Lambert SD, Heinrichs B, Weekers F et al (2014) Effect of encapsulated nanoparticles on thermophillic anaerobic digestion, 19th National symposium on applied biological sciences, Gembloux, Belgium. https://orbi.uliege.be/handle/2268/169020
13. Abdelsalam E, Samer M, Attia YA, Abdel-Hadi MA, Hassan HE, Badr Y (2016) Comparison of nanoparticles effects on biogas and methane production from anaerobic digestion of cattle dung slurry. Renewable Energy 87:592–598
14. Abdelsalam E, Samer M, Attia YA, Abdel-Hadi MA, Hassan HE, Badr Y (2017) Effect of Co and Ni on biogas and methane production from anaerobic digestion of slurry. Energy Conv Manag 141:108–119
15. Otero-González L, Field JA, Sierra-Alvarez R (2014) Inhibition of anaerobic waste- water treatment after long-term exposure to low levels of CuO nanoparticles. Water Res 58:160–168
16. Luna-delRiscoa M, Orupõlda K, Dubourguier H-C (2011) Particle size effect of CuO and ZnO on biogas and methane production during anaerobic digestion. J Hazard Mater 189:603–608
17. Gonzalez-Estrella J, Sierra-Alvarez R, Field JA (2013) Toxicity assessment of inorganic nanoparticles to acetoclastic and hydrogenotrophic methanogenic activity in anaerobic granular sludge. J Hazard Mater 260:278–285
18. Yu HQ, Fang HHP (2001) Inhibition by chromium and cadmium of anaerobic acidogenesis. Water Sci Tech 43:267–274
19. Codina JC, Munoz MA, Cazorla FM, Perez-Garcıa A, Morinigo MA, De Vicente A (1998) The inhibition of methanogenic activity from anaerobic domestic sludges as a simple toxicity bioassay. Water Res 32:1338–1342
20. Yue Z-B, Yu H-Q, Wang Z-L (2007) Anaerobic digestion of cattail with rumen culture in the presence of heavy metals. Bioresource Tech 98:781–786
21. Hingston JA, Collins CD, Murphy RJ, Lester JN (2001) Leaching of chromated copper arsenate wood preservatives: a review. Environ Pollut 111:53–66
22. Soliman W, Yamani RN, Sabry D, Mostafa A (2021) Stainless steel quantum dots and its resonance fluorescence impact as new therapeutic agents for Laryngeal carcinoma treatment: In vitro study. Opt Laser Tech 142:107263
23. Soliman W (2020) Laser ablation of stainless steel in water and hexane: characterization of surface modification and nanoparticles for various applications. Surf Eng Appl Electrochem 56:133–139
24. Sliem MA, El-Ansary S, Soliman W, Badr Y (2022) Enhancing biogas production of cow dung during anaerobic digestion using nanoferrites. Biomass Conv Bioref 12:4139–4146. https://doi.org/10.1007/s13399-021-01683-8
25. Soliman W, El-Ansary S, Badr Y (2018) Impact of liquid medium on laser ablation mechanism: surface heating and cooling, lasers Manuf. Mater Process 5:430–438
26. Mollah S, Henley SJ, Giusca CE, Silva SRP (2010) Photo-chemical synthesis of iron oxide nanowires induced by pulsed laser ablation of iron powder in liquid media. Integr Ferroelectr 119:45–54
27. Henley J, Mollah S, Giusca CE, Silva SRP (2009) Laser-induced self-assembly of iron oxide nanostructures with controllable dimensionality. J Appl Phys 106:064309
28. Soliman W, El-Ansary S, Badr Y (2017) Optical characterization of one-step synthesis of ternary nanoalloy bylaser ablation of stainless steel target in hexane. Optics Laser Tech 97:41–45
29. Hirsch LR, Stafford RJ, Bankson JA, Sershen SR, Rivera B, Price RE, Hazle JD, Halas NJ, West JL (2003) Nanoshell-mediated near-infrared thermal therapy of tumors under magnetic resonance guidance. Proc Natl Acad Sci U S A 100:13549–13554
30. Gedefaw M (2015) Biogas production from cow dung and food waste. Glob J Pollut Hazard Waste Manage 3:103–108
31. Abdelwahab TAM, Mohanty MK, Sahoo PK et al (2022) Impact of iron nanoparticles on biogas production and effluent chemical composition from anaerobic digestion of cattle manure. Biomass Conv Bioref 12:5583–5595. https://doi.org/10.1007/s13399-020-00985-7
32. Akar AA, Seif R, Taha MM, Ismail AAM, Allam NK (2023) Production of high-quality biogas using recycled trimetallic nanoparticles from electronic waste. Mater Today Sustain 24:100477. https://doi.org/10.1016/j.mtsust.2023.100477
33. Kaskun S, Çalhan R, Akinay Y (2023) Enhancement of biogas production using SnO2 nanoparticle-doped mica catalyst. Biomass Conv Bioref 13:7239–7246. https://doi.org/10.1007/s13399-021-01983-z